

FREE AND FORCED NONLINEAR VIBRATION OF STEEL FRAMES WITH SEMI-RIGID CONNECTIONS

Andréa R.D. Silva*, Ricardo A.M. Silveira*, Alexandre S. Galvão** and Paulo B. Gonçalves***

* Department of Civil Engineering, School of Mines, Federal University of Ouro Preto
e-mails: andreadiassilva@yahoo.com.br, ricardo@em.ufop.br

** Fluminense Federal University, Campus of Volta Redonda
e-mail: asgalvao@vm.uff.br

*** Department of Civil Engineering, Pontifical Catholic University of Rio de Janeiro
e-mail: paulo@puc-rio.br

Keywords: Structural stability, Nonlinear vibration, Pre-loaded structures, Semi-rigid connections.

***Abstract.** The increasing slenderness of structural frames makes them more susceptible to vibration and buckling problems. The present work studies the free and forced nonlinear vibrations of steel frames with semi-rigid connections. Special attention is given to the influence of static pre-load on the natural frequencies and mode shapes, nonlinear frequency-amplitude relations, and resonance curves. These results are obtained using a nonlinear finite element program for static and dynamic analysis of steel frames. Two structural systems with important practical applications are analyzed, namely: a shallow arch and a pitched-roof steel frame. The results show the importance of the static pre-load and the stiffness of the semi-rigid connection on the buckling and vibration characteristics of these structures.*

1 INTRODUCTION

During the last ten years, studies and research have concentrated on the vibration problems of structures subjected to dynamic loads. This has brought significant advance in the civil construction industry, where new techniques and materials have been either developed or improved. Maybe the largest contributor to this advance is the use of more precise numerical computational tools, whose models permit realistic simulation and resolution of structural problems. Today, with all these advances, it is possible to design more streamline and flexible buildings. However, this makes them more susceptible to the effects of dynamic actions, creating ever-growing problems. This can be observed in the technical literature where failures involving from localized damage to total structural collapse are described. There are also cases of vibration-related discomfort experienced by users, even when there is no structural damage. Because of this, nonlinear dynamic analysis of slender steel structures is ever more relevant.

In most reports on linear and nonlinear structural vibrations, it is assumed that the system is free of loading and that a dynamic load is suddenly applied for a given time duration. This may lead to erroneous results when slender structures susceptible to buckling are investigated. Simitsep [1] discussed the effects of static preloading on the dynamic stability of structures. The effect of static pre-load on the structure's dynamics has also been studied by Wu and Thompson [2], and Zeinoddini et al. [3], among others. The interplay between buckling and vibration has been the subject of some previous papers [3-6]. These studies show that compressive stress states decrease the structure's natural frequencies and may even change the mode shapes associated with the lowest natural frequencies [5]. They also decrease the effective stiffness and consequently increase the vibration amplitudes, which may weaken or even damage the structure. Finally, shifting the natural frequencies to a lower frequency range may increase resonance

problems due to environmental loads. Solutions to these vibration problems usually require the use of costly control systems or changes in the structural design [7].

Transient linear and nonlinear analysis of beams and frames with semi-rigid connections, as well as the study of vibratory problems associated with these structural systems, can also be found in publications by Chan and Chui [8], Sophianopoulos [9] and Sekulovic *et al.* [10].

The aim of the present work is to conduct, using the nonlinear finite element program CS-ASA (Computational System for Advanced Structural Analysis, Silva [11]), a dynamic analysis of steel frames and to study the influence of second-order effects generated by large displacements and rotations, connection flexibility, and pre-stress states on the nonlinear response of slender steel structures.

2 THE FREE VIBRATION PROBLEM

The geometric nonlinear finite element formulation for frames with rigid connections implemented in the CS-ASA is based on work by Yang and Kuo [12]. The consideration of semi-rigid connections is based on the formulations proposed by Chan and Chui [8] and Sekulovic *et al.* [10].

In the finite element method context, the equilibrium of any structural system can be expressed as:

$$\mathbf{F}_i(\mathbf{U}) = \lambda \mathbf{F}_r \quad (1)$$

where \mathbf{F}_i is the internal forces vector, function of the generalized displacement vector \mathbf{U} , λ is a load factor, and \mathbf{F}_r is a fixed reference vector defining the direction and distribution of the applied loads.

To obtain the nonlinear equilibrium path of a structure, an incremental technique for the response is used to solve the equation system (1). This procedure basically consists of calculating a sequence of incremental displacements, $\Delta \mathbf{U}_i$, that correspond to a sequence of given load increments, $\Delta \lambda_i$. However, as \mathbf{F}_i is a nonlinear function of \mathbf{U} , the estimated solution for the problem (predicted solution: $\Delta \lambda^0, \Delta \mathbf{U}^0$) for each load step normally does not satisfy (1). Consequently, a residual force vector \mathbf{g} is defined. If this residual force vector does not satisfy the convergence criteria, a new estimate for \mathbf{U} is obtained.

The vibration frequency analysis is crucial in the stability analysis of structural systems with strongly nonlinear equilibrium paths, and the dynamic stability criterion can be used to define the type of the equilibrium configuration. So, the vibration frequencies and the corresponding modes of vibration in a structure can be obtained by solving the following eigenvalue problem:

$$(\mathbf{K} - \omega^2 \mathbf{M}) \boldsymbol{\phi} = \mathbf{0} \quad (2)$$

where \mathbf{K} is the tangent stiffness matrix of the structural system, \mathbf{M} is the mass matrix, ω is the natural frequency, and $\boldsymbol{\phi}$ is the vibration mode vector. The influence of static preloading and semi-rigid connections on structural system vibration modes and natural frequencies is studied here. The static preloading effect is related with the presence of axial force on bars and its inclusion is made considering the geometric stiffness matrix as part of \mathbf{K} in (2); the semi-rigid connections influence is included evaluating the joint stiffness at the assumed load level and consequently changing the linear stiffness matrix. However, as the geometric nonlinearity and the connection flexibility effects are considered, the solution to the equation (2) cannot be obtained directly. Table 1 illustrates the step-by-step numerical procedures for solving the static nonlinear problem and, subsequently, calculating the natural frequencies and vibration modes of the loaded structure. This algorithm illustrates that for each load step the equation (2) is solved considering the structural stiffness change due the initial stress (preloading).

3 NONLINEAR TRANSIENT ANALYSIS

The nonlinear time response of the structure can be obtained by solving the following set of discrete equations of motion:

$$\mathbf{M}\ddot{\mathbf{U}} + \mathbf{C}\dot{\mathbf{U}} + \mathbf{F}_i(\mathbf{U}) = \lambda(t)\mathbf{F}_r \quad (3)$$

Table 1: Numerical strategy for free vibration analysis of pre-loaded frames.

<p>1. Input the material and geometric properties of the frame</p> <p>2. Obtain the reference force vector \mathbf{F}_r</p> <p>3. Displacement and load parameter in the actual equilibrium configuration: ${}^t\mathbf{U}$ and ${}^t\lambda$</p> <p>4. INCREMENTAL TANGENT SOLUTION: $\Delta\lambda^0$ and $\Delta\mathbf{U}^0$</p> <p>4a. Calculate the tangent stiffness matrix \mathbf{K}</p> <p>4b. Solve: $\delta\mathbf{U}_r = \mathbf{K}^{-1}\mathbf{F}_r$</p> <p>4c. Define $\Delta\lambda^0$ with a determined strategy for the load increment [11]</p> <p>4d. Calculate: $\Delta\mathbf{U}^0 = \Delta\lambda^0\delta\mathbf{U}_r$</p> <p>4e. Update the variables in the new equilibrium configuration $t + \Delta t$: ${}^{(t+\Delta t)}\lambda = {}^t\lambda + \Delta\lambda^0$ and ${}^{(t+\Delta t)}\mathbf{U} = {}^t\mathbf{U} + \Delta\mathbf{U}^0$</p> <p>5. NEWTON-RAPHSON ITERATION: $k = 1, 2, 3, \dots$</p> <p>5a. Calculate the internal forces vector: ${}^{(t+\Delta t)}\mathbf{F}_i^{(k-1)} = {}^t\mathbf{F}_i + \mathbf{K}\Delta\mathbf{U}^{(k-1)}$</p> <p>5b. Calculate the unbalanced forces vector: $\mathbf{g}^{(k-1)} = {}^{(t+\Delta t)}\lambda^{(k-1)}\mathbf{F}_r - {}^{(t+\Delta t)}\mathbf{F}_i^{(k-1)}$</p> <p>5c. Verify the convergence: $\ \mathbf{g}^{(k-1)}\ / ({}^{(t+\Delta t)}\lambda^{(k-1)}\mathbf{F}_r) \leq \xi$, with ξ being the tolerance factor.</p> <p>YES: Stop the iteration cycle and go to item 5h</p> <p>5d. Obtain $\delta\lambda^k$ using an iteration strategy [11]</p> <p>5e. Determine $\delta\mathbf{U}^k = \delta\mathbf{U}_g^k + \delta\lambda^k \delta\mathbf{U}_r^k$, with $\delta\mathbf{U}_g^k = -\mathbf{K}^{-1(k-1)}\mathbf{g}^{(k-1)}$ and $\delta\mathbf{U}_r^k = \mathbf{K}^{-1(k-1)}\mathbf{F}_r$</p> <p>5f. Update the load parameters, λ, and the nodal displacement vector, \mathbf{U}:</p> <p>a) <i>Increments:</i> $\Delta\lambda^k = \Delta\lambda^{(k-1)} + \delta\lambda^k$ and $\Delta\mathbf{U}^k = \Delta\mathbf{U}^{(k-1)} + \delta\mathbf{U}^k$</p> <p>b) <i>Totals:</i> ${}^{(t+\Delta t)}\lambda^k = {}^t\lambda + \Delta\lambda^k$ and ${}^{(t+\Delta t)}\mathbf{U}^k = {}^t\mathbf{U} + \Delta\mathbf{U}^k$</p> <p>5g. Return to step 5</p> <p>5h. Determine the natural frequencies and the associated vibrations modes:</p> <p>a) Update the tangent stiffness matrix \mathbf{K} and the mass matrix \mathbf{M}</p> <p>b) Decompose \mathbf{M} by the the Cholesky method: $\mathbf{M} = \mathbf{S}^T\mathbf{S}$ and obtain $\mathbf{A} = (\mathbf{S}^{-1})^T\mathbf{K}\mathbf{S}^{-1}$</p> <p>c) Solve the eigenvalue problem $\mathbf{A}\mathbf{X} = \lambda\mathbf{X}$ by using the Jacobi Method, obtaining the eigenvalues (ω^2) and the eigenvectors (vibration modes)</p> <p>6. CONSIDER NEW LOAD INCREMENT AND RETURN TO STEP 4</p>

where \mathbf{M} and \mathbf{C} are the mass and viscous damping matrices, respectively, and \mathbf{F}_i is the internal force vector that depends on the displacement vector \mathbf{U} of the system, $\dot{\mathbf{U}}$ and $\ddot{\mathbf{U}}$ are the velocity and acceleration vectors, respectively, and $\lambda(t)\mathbf{F}_r$ is the external excitation vector.

The solution of the nonlinear dynamic system (3) can be obtained through a time integration algorithm together with adaptive strategies for the automatic increment of the time step. The numerical methodology used here is presented in table 2. Details of the nonlinear dynamic formulation as well as the computational program are found in Silva [11].

3.1 Nonlinear Vibration Analysis

The nonlinear frequency-amplitude relation provides fundamental information on the nonlinear vibration analysis of any structural system, and it gives a good indication of the type (hardening or softening) and degree of nonlinearity of the system. Here the methodology proposed by Nandakumar and Chatterjee [13] is used to obtain this relation using the finite element method. First, the nonlinear equations of motion are numerically integrated (table 2), and the time response of the slightly damped system is obtained for a chosen node. Then, the maximum amplitude and corresponding period between two consecutive positive peaks are computed at each cycle. Consider two successive peaks at times $t_{(i)}$ and $t_{(i+1)}$ (see figure 1). Let their average value be d_{1m} and let the trough between these two positive peaks be d_2 . Then, the amplitude can be defined by:

$$d_i = 1/2 \left(d_{1m(i)} + |d_{2(i)}| \right) \quad (4)$$

and the frequency as $f_i = 1/T_i$, with $T_i = t_{(i+1)} - t_{(i)}$. The resulting amplitude and frequency values are plotted to give the frequency-amplitude relation. To obtain the peak amplitudes with the necessary accuracy, a small time step must be imposed in the integration process. In addition, a large number of elements are necessary to describe accurately the large amplitude response of the structure.

Table 2: Numerical strategy for nonlinear transient analysis.

-
1. Input the material and geometric properties of the frame, and obtain the force vector \mathbf{F}_r
 2. Start the initial displacement, velocity and acceleration vectors, ${}^0\mathbf{U}$, ${}^0\dot{\mathbf{U}}$ and ${}^0\ddot{\mathbf{U}}$
 3. **FOR EACH TIME STEP $t + \Delta t$**
 - 3a. Derive the tangent stiffness, mass and damping matrices: \mathbf{K} , \mathbf{M} , and \mathbf{C}
 - 3b. Using Newmark parameters β and γ , calculate the constants:

$$a_0 = 1/(\beta\Delta t^2); a_1 = \gamma/(\beta\Delta t); a_2 = 1/(\beta\Delta t); a_3 = 1/(2\beta) - 1; a_4 = \gamma/\beta - 1;$$

$$a_5 = \Delta t(\gamma/(2\beta) - 1); a_6 = a_0; a_7 = -a_2; a_8 = -a_3; a_9 = \Delta t(1 - \gamma); a_{10} = \alpha\Delta t$$
 - 3c. Form the effective stiffness matrix: $\hat{\mathbf{K}} = \mathbf{K} + a_0\mathbf{M} + a_1\mathbf{C}$
 - 3d. Calculate: $\hat{\mathbf{F}} = ({}^{t+\Delta t})\lambda\mathbf{F}_r + \mathbf{M}(a_2 {}^t\dot{\mathbf{U}} + a_3 {}^t\ddot{\mathbf{U}}) + \mathbf{C}(a_4 {}^t\dot{\mathbf{U}} + a_5 {}^t\ddot{\mathbf{U}}) - {}^t\mathbf{F}_i$
 - 3e. Solve for displacement increments: $\hat{\mathbf{K}}\Delta\mathbf{U} = \hat{\mathbf{F}}$
 4. **NEWTON-RAPHSON ITERATION: $k = 1, 2, 3, \dots$**
 - 4a. Evaluate the approximation of the acceleration, velocities and displacements:

$$({}^{t+\Delta t})\ddot{\mathbf{U}}^k = a_0\Delta\mathbf{U}^k - a_2 {}^t\dot{\mathbf{U}} - a_3 {}^t\ddot{\mathbf{U}}; ({}^{t+\Delta t})\dot{\mathbf{U}}^k = a_1\Delta\mathbf{U}^k - a_4 {}^t\dot{\mathbf{U}} - a_5 {}^t\ddot{\mathbf{U}}; ({}^{t+\Delta t})\mathbf{U}^k = {}^t\mathbf{U} + \Delta\mathbf{U}^k$$
 - 4b. Update the geometry of the frame
 - 4c. Evaluate the internal forces vector: $({}^{t+\Delta t})\mathbf{F}_i^k = {}^t\mathbf{F}_i + \mathbf{K}\Delta\mathbf{U}^k$
 - 4d. Form: $({}^{t+\Delta t})\mathbf{R}^{(k+1)} = ({}^{t+\Delta t})\lambda\mathbf{F}_r - (\mathbf{M}({}^{t+\Delta t})\ddot{\mathbf{U}}^k + \mathbf{C}({}^{t+\Delta t})\dot{\mathbf{U}}^k + ({}^{t+\Delta t})\mathbf{F}_i^k)$
 - 4e. Solve for the corrected displacement increments $\hat{\mathbf{K}}\delta\mathbf{U}^{(k+1)} = ({}^{t+\Delta t})\mathbf{R}^{(k+1)}$
 - 4f. Evaluate the corrected displacement increments: $\Delta\mathbf{U}^{(k+1)} = \Delta\mathbf{U}^k + \delta\mathbf{U}^{(k+1)}$
 - 4g. Check the convergence of the iteration process:

$$\|\Delta\mathbf{U}^{(k+1)}\| / \|{}^t\mathbf{U} + \Delta\mathbf{U}^{(k+1)}\| \leq \xi, \text{ where } \xi \text{ is a tolerance factor} \quad \text{NO: Go to 4}$$
 - 4h. Calculate the acceleration, velocities and displacements at time $t + \Delta t$

$$({}^{t+\Delta t})\ddot{\mathbf{U}}^{(k+1)} = a_0\Delta\mathbf{U}^{(k+1)} - a_2 {}^t\dot{\mathbf{U}} - a_3 {}^t\ddot{\mathbf{U}}; ({}^{t+\Delta t})\dot{\mathbf{U}}^{(k+1)} = a_1\Delta\mathbf{U}^{(k+1)} - a_4 {}^t\dot{\mathbf{U}} - a_5 {}^t\ddot{\mathbf{U}}$$

$$({}^{t+\Delta t})\mathbf{U}^{(k+1)} = {}^t\mathbf{U} + \Delta\mathbf{U}^{(k+1)}$$
 5. **FOR THE NEXT TIME STEP**
 - 5a. Evaluate the internal forces vector: $({}^{t+\Delta t})\mathbf{F}_i^{(k+1)} = {}^t\mathbf{F}_i + \mathbf{K}\Delta\mathbf{U}^{(k+1)}$
 - 5b. Select a new time step Δt (adaptive strategy)
-

3.2 Resonance Analysis

Low-dimensional numerical models employ relatively easy techniques for obtaining nonlinear resonance curves. In contrast, it is computationally difficult to obtain these curves for structural systems with a large number of degrees of freedom. Here, a simple repetitive procedure coupled with the integration method is implemented, which consists in giving constant excitation-frequency increments $\Delta\Omega$ and, for each incremental step, integrate the differential equations of motion during N harmonic excitation cycles. The response of the initial cycles associated with the short transient response is

dismissed, and the maximum amplitude of the steady-state solution is plotted as a function of the forcing frequency. Of course, this brute force method is unable to obtain unstable branches of resonance curves or all co-existing stable solutions.

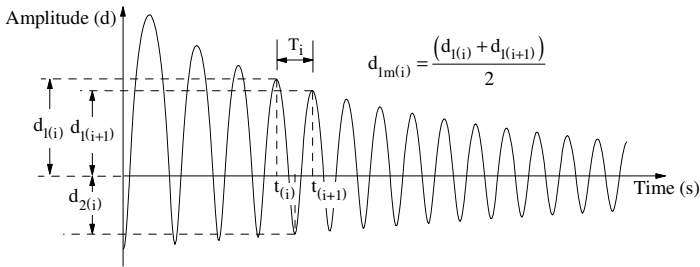


Figure 1: Procedure for obtaining the displacements d_i and the frequency f_i .

4 NUMERICAL EXAMPLES

4.1 Shallow arch

Slender arches are structures that may present, depending on the support conditions and the type and intensity of loading, a highly nonlinear structural behavior. The dynamic response of these arches has been extensively analyzed due to their practical applications. This subsection analyzes the sinusoidal arch under vertical distributed load P presented in figure 2 [14].

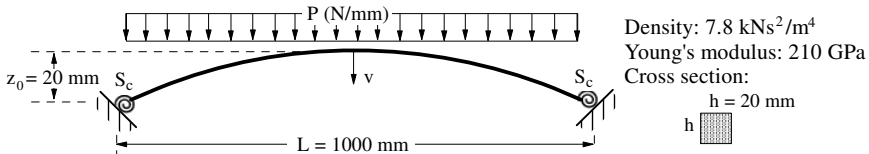


Figure 2: Arch with semi-rigid joints: geometry and loading.

Figure 3a shows the arch equilibrium paths for different support rotation stiffness S_c . For more flexible connections the presence of two limits points in the equilibrium path is observed which disappears as the stiffness of the supports increase. The curve obtained for the simply supported arch, $S_c = 0$, is compared with the analytical solution provided by Bergan [14].

Figure 3b shows the nonlinear relation between the load P and the lowest natural frequency considering increasing support stiffness. The curves show not only the influence of static pre-loading in the natural frequencies, but also indicate, in accordance with the dynamic instability criterion, the stable and unstable equilibrium configurations along of the equilibrium paths. Based on this criterion, the unstable parts ($\omega^2 < 0$) are located between the points A_1, A_2, B_1, B_2, C_1 and C_2 .

Figure 4a illustrates the nonlinear relation between the frequency and the free vibration amplitude of the arch. To obtain such a response, a damping rate equal to 0.01 and a constant time step equal to 10^{-5} is considered. Three different support conditions are studied: pinned ($S_c = 0$), perfectly rigid ($S_c \rightarrow \infty$) and semi-rigid ($S_c = 10 EI/L$). In all three situations, the arch displays initially hardening behavior, i.e., the frequency increases with increasing vibration amplitudes. However, for large vibration amplitudes a softening behavior is observed which is more pronounced for the pinned arch. The natural frequencies, in Hz, for each arch (rigid, semi-rigid and pinned) is indicated by a dashed line. The dynamic response of the pinned arch under a uniformly distributed harmonic excitation, $P = A_p \sin(\Omega t)$, is investigated next. Figure 4b shows the variation of the maximum and minimum amplitude of the steady-state response, v/z_0 , as a function of the forcing frequency parameter Ω/ω_a ($\omega_a = 238.4$ rad/s) for different amplitudes of the

harmonic excitation, A_p/h . When the excitation magnitude increases, the resonance peaks move sharply to the lower frequency range, indicating a strong softening behavior in agreement with the frequency-amplitude relation shown in figure 4a. This behavior is also compatible with the type of nonlinearity observed in the system's static solution. As is typical of nonlinear systems, the resonance curve begins to bend at $A_p/h = 0.4$ in a region of low frequencies, which produces more than one permanent solution for the same frequency value. When the magnitude of excitation reaches $A_p/h = 0.5$, the amplitude increases considerably in the low frequency region up to the point where the arch loses stability and inverts its concavity.

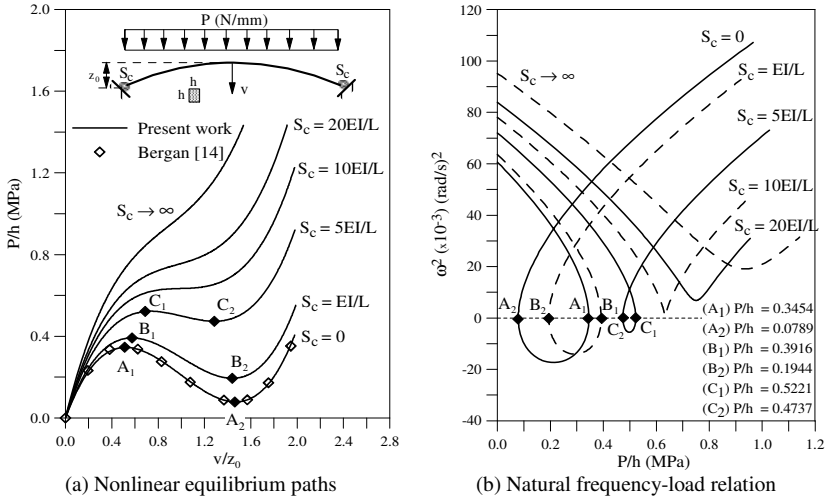


Figure 3: Static analysis and influence of static pre-load on the lowest natural frequency.

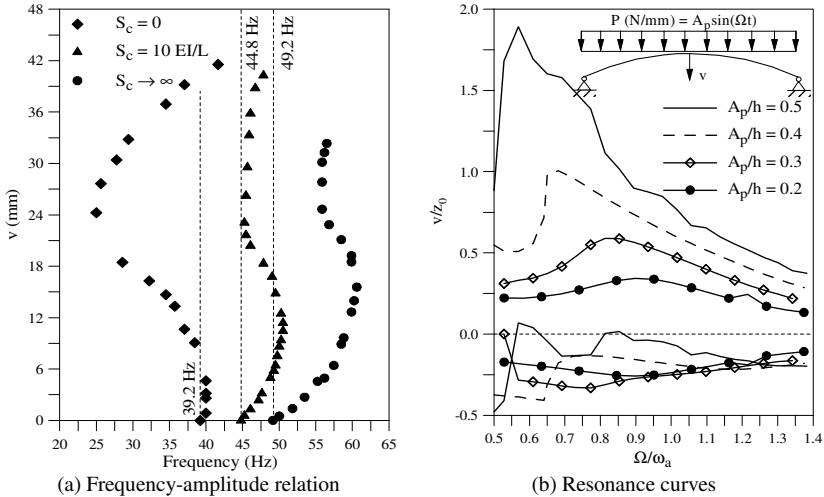


Figure 4: Nonlinear vibration and resonance analysis for selected values of the connection stiffness S_c .

4.2 Pitched-roof steel frame

The numerical strategy developed is now applied to the analysis of a pitched-roof frame with beam-column flexible joints, as shown in figure 5. Twenty finite elements are used here to model the structure.

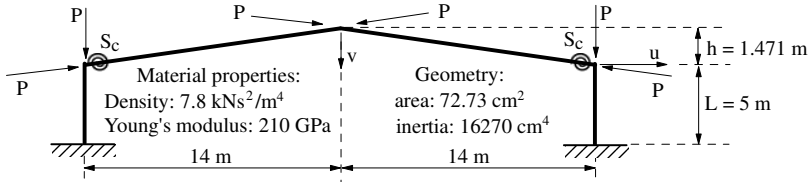


Figure 5: Pitched-roof frame: geometry and loading.

Figure 6a shows the nonlinear equilibrium paths for increasing values of the joint stiffness S_c . The nonlinear relation between the load and the natural frequencies for different values of joint stiffness is given in figure 6b. The applied load is non-dimensionalized by the Euler load $P_e = \pi^2 EI/L^2$, and the frequencies are non-dimensionalized by the lowest free vibration frequency of the unloaded frame with rigid connections, $\omega_0 = 23.912$ rad/s. The non-linear paths display a limit load (points A, B, C and D) as shown in figure 6a. Figure 6b shows the variation of the lowest natural frequency with the applied load. The almost linear relation between the square of the frequency of the pre-loaded structure and the applied load can be used to evaluate the buckling load through at least two experimental values of the lowest frequency for two small load levels. Finally, figure 6c shows the frequency-amplitude relation of the pitched-roof for three selected values of the beam-column joints stiffness. The relation is almost linear for small-to-medium amplitude oscillations and of the softening type when very large vibration amplitudes occur, which is outside the range of practical applications.

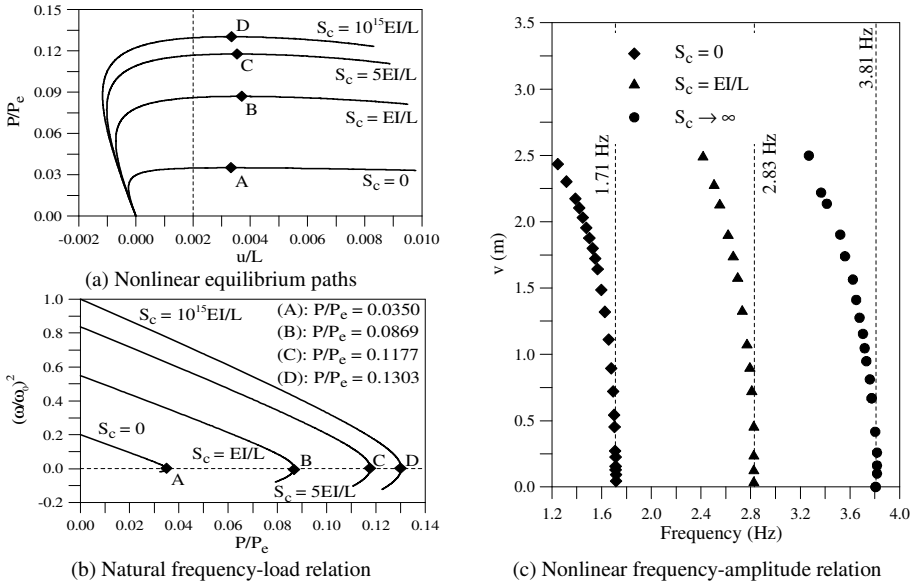


Figure 6: Static and vibration analysis of the pitched-roof steel frame.

5 CONCLUSION

The results presented in this paper indicate that the precise evaluation of the connection stiffness, a key point in the design of steel structures, is essential for the calculation of critical conditions. This is particularly important for practical application where damage usually occurs at the connections, decreasing their stiffness and radically changing the nonlinear behavior of the frame. The results also

indicate that the loss of stiffness of a connection during the service life of the structure may significantly affect the structural behavior under both static and dynamic loads. This is in agreement with the literature describing structural failures due to support deterioration. In some cases, a slow decrease in the joint stiffness S_c value can change the overall stiffness of the structure and its dynamic characteristics, and this can only be detected and quantified by detailed nonlinear behavior analyses of the structure. Finally, the results also showed the influence of the static pre-loading on the natural frequencies and the nonlinear frequency-amplitude relation of the analyzed structural systems.

Acknowledgment

The authors wish express their gratitude to CAPES, CNPq, FAPEMIG and FAPERJ for the financial support received in the development of this research.

REFERENCES

- [1] Simitsets, G.J., "Effect of static preloading on the dynamic stability of structures", *AIAA Journal*, **21**(8), 1174-1180, 1983.
- [2] Wu, T.X. and Thompson, D.J., "The effects of local preload on the foundation stiffness and vertical vibration of railway track", *Journal of Sound and Vibration*, **219**(5), 881-904, 1999.
- [3] Zeinoddini, M., Harding, J.E., Parke, G.A.R., "Dynamic behaviour of axially pre-loaded tubular steel members of offshore structures subjected to impact damage", *Ocean Engineering*, **26**(10), 963-978, 1999.
- [4] Gonçalves, P.B., "Axisymmetric vibrations of imperfect shallow spherical caps under pressure loading", *Journal of Sound and Vibration*, **174**(2), 249-260, 1994.
- [5] Nieh, K.Y., Huang, C.S., Tseng, Y.P., "An analytical solution for in-plane free vibration and stability of loaded elliptic arches", *Computers & Structures*, **81**(13), 311-1327, 2003.
- [6] Xu, R. and Wu, Y-F., "Free vibration and buckling of composite beams with interlayer slip by two-dimensional theory", *Journal of Sound and Vibration*, **313**(3-5), 875-890, 2008.
- [7] Soong, T.T. and Dargush, G.F., *Passive Energy Dissipation Systems in Structural Engineering*, John Wiley & Sons, Chichester, 1997.
- [8] Chan, S.L. and Chui, P.P.T., *Nonlinear Static and Cyclic Analysis of Steel Frames with Semi-Rigid Connections*, Elsevier, Kidlington, UK, 2000.
- [9] Sophianopoulos, D.S., "The effect of joint flexibility on the free elastic vibration characteristics of steel plane frames", *Journal of Constructional Steel Research*, **59**(8), 995-1008, 2003.
- [10] Sekulovic, M., Salatic, R., Nefovska, M., "Dynamic analysis of steel flexible connections", *Computers & Structures*, **80**, 935-955, 2002.
- [11] Silva, A.R.D., *Computational System for Advanced Static and Dynamic Analysis of Steel Structures*, D.Sc. Thesis, PROPEC/Deciv/UFOP, Ouro Preto, Brazil, 2009 (in Portuguese).
- [12] Yang, Y.B. and Kuo, S.B., *Theory and Analysis of Nonlinear Framed Structures*, Prentice Hall, 1994.
- [13] Nandakumar, K. and Chatterjee, A., "Resonance, parameter estimation, and modal interactions in a strongly nonlinear benchtop oscillator", *Nonlinear Dynamics*, **40**, 149-167, 2005.
- [14] Bergan, P.G., "Solution algorithms for nonlinear structural problems", *Computers & Structures*, **12**, 497-509, 1980.